NANO LETTERS

LETTER

pubs.acs.org/NanoLett

Thermoelectricity in Fullerene−Metal Heterojunctions

Shannon K. Yee,[†,∥] Jonathan A. Malen,[†,∥,⊥] Arun Majumdar,[*,‡] and Rachel A. Segalman[*,§]

[†]Department of Mechanical Engineering, University of California, Berkeley, California 94720, United States

[‡]United States Department of Energy, ARPA-E, Washington, DC 20585, United States

[§]Department of Chemical and Biomolecular Engineering, University of California, Berkeley, California 94720, United States

Supporting Information

ABSTRACT: Thermoelectricty in heterojunctions, where a single-molecule is trapped between metal electrodes, has been used to understand transport properties at organic−inorganic interfaces.[1] The transport in these systems is highly dependent on the energy level alignment between the molecular orbitals and the Fermi level (or work function) of the metal contacts. To date, the majority of single-molecule measurements have focused on simple small molecules where transport is dominated through the highest occupied molecular orbital.[2,3] In these systems, energy level alignment is limited by the absence of electrode materials with low Fermi levels (i.e., large work functions). Alternatively, more controllable alignment between molecular orbitals and the Fermi level can be achieved with molecules whose transport is dominated by the lowest unoccupied molecular orbital (LUMO) because of readily available metals with lower work functions. Herein, we report molecular junction thermoelectric measurements of fullerene molecules (i.e., C_{60}, PCBM, and C_{70}) trapped between metallic electrodes (i.e., Pt, Au, Ag). Fullerene junctions demonstrate the first strongly n-type molecular thermopower corresponding to transport through the LUMO, and the highest measured magnitude of molecular thermopower to date. While the electronic conductance of fullerenes is highly variable, due to fullerene's variable bonding geometries with the electrodes, the thermopower shows predictable trends based on the alignment of the LUMO with the work function of the electrodes. Both the magnitude and trend of the thermopower suggest that heterostructuring organic and inorganic materials at the nanoscale can further enhance thermoelectric performance, therein providing a new pathway for designing thermoelectric materials.

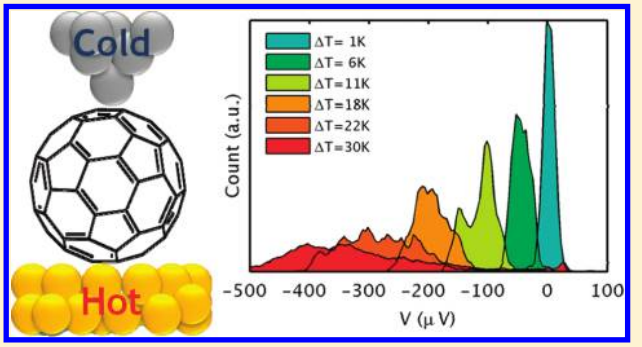

KEYWORDS: Molecular thermopower, fullerene conductivity, fullerene thermoelectricity, C60 Seebeck

The efficiency of thermoelectrics depends on a combination of material properties quantified by the thermoelectric figure of merit $ZT = S^2\sigma T/k$, where S is thermopower, σ is electronic conductivity, and k is thermal conductivity. While S and σ are primarily based on electronic structure, k typically has both electron and phonon contributions. During the past decade, gains in ZT have been realized through a reduction in the phonon contribution to k by introducing interfaces through the presence of nanostructuring. In bulk semiconductors S and σ are opposing functions of doping concentration[4] and a compromise that optimizes $S^2\sigma$ is typically sought. Systems that can independently optimize S and σ are rare and Mahan and Sofo[5] argued that a system with discrete electronic density of states (e.g., Dirac delta peaks) could possess the highest ZT. Single-molecule heterojunctions, where a single-molecule is trapped between metal electrodes, are one such system where a discrete density of states exists at the frontier molecular orbitals (MOs). Understanding and leveraging these heterojunctions could open new pathways for enhanced thermoelectric performance, impossible in bulk semiconductors due to their fundamentally different transport properties.

Electronic transport in single-molecule heterojunctions can be described by the Landauer formalism,[2] where charge carriers transmit between electrodes 1 and 2, through a molecular bridge (Figure 1), with an energy-dependent probability defined by the transmission function $\tau(E)$ (Figure 5b). The discrete MOs hybridize with the continuum electronic states in the metals and a continuous transmission probability with Lorentzian like peaks at energies related to the MOs form. The electrons that are free to participate in transport have energies near the chemical potential and the chemical potential lies between the frontier MOs. The electronic conductance, G, and thermopower, S, are related to this transmission function and thus the relative alignment of the Fermi level, E_F, and the highest occupied molecular orbital (HOMO) and lowest unoccupied molecular orbital (LUMO). Specifically, the electronic conductance of the junction is proportional to $\tau(E)$ evaluated at the chemical potential, μ

$$G = \frac{2e^2}{h}\tau(E)|_{E=\mu} \quad (1)$$

Received: May 4, 2011
Revised: August 29, 2011

   dx.doi.org/10.1021/nl2014839 | *Nano Lett.* XXXX, XXX, 000–000

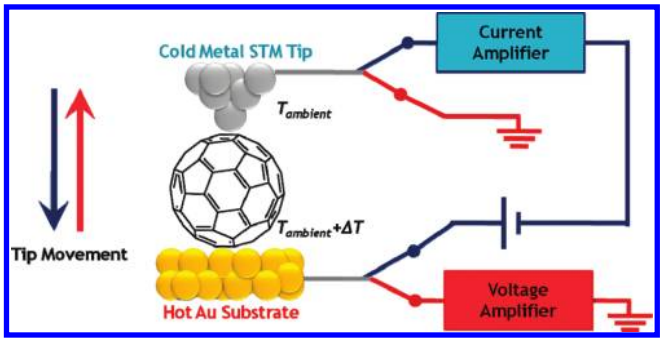

Figure 1. Measurement setup. (a) Schematic of the experimental setup for measuring conductance and thermopower with a modified scanning tunneling microscopy (STM) break junction. For conductance, a voltage bias is applied between the tip and substrate and the conductance is determined using a current amplifier. The STM tip contacts the substrate and traps fullerene molecules. For thermopower, fullerene molecules are trapped between the STM tip held at ambient temperature and a heated Au substrate held at ΔT above the ambient temperature. As the STM tip approaches a voltage bias is applied between the tip and substrate, and conductance is monitored. Once a threshold conductance is reached, indicating formation of a molecular junction, the tip is withdrawn. During the withdrawal sequence, a switch disconnects the voltage bias and current amplifier in favor of a voltage amplifier. The induced thermoelectric voltage V is measured as the tip withdraws but before the junction breaks.

where e is the electron charge and h is Planck's constant. Similarly, the thermopower of a molecular junction can be related to $\tau(E)$

$$S = -\frac{\pi^2 k_B^2 T}{3e}\left(\frac{1}{\tau(E)}\frac{\partial\tau(E)}{\partial E}\right)_{E=\mu} \quad (2)$$

where k_B is Botlzmann's constant and T is the average temperature of the junction. In other words, the thermopower is related to the slope of the transmission function at μ. Closer inspection of the transmission function illustrates that near a transmission peak, the slope (and thus the S) and the transmission probability (and thus the G) are maximum. In this manner, it is clear to see that under the Landauer description of transport both σ and S can be concurrently optimized. Therefore, optimizing σ and S is simply a matter of aligning the MOs with the Fermi level of electrodes.[2,6]

Alignment with MOs can be achieved in two ways: (i) by altering the MOs of the molecule by adding electron donating or withdrawing substituents or (ii) by varying the electrode material. Previous molecular junction measurements[2,3] have focused on molecules, such as phenylenedithiol, whose transport is dominated through the HOMO. It has previously been demonstrated that for phenylene derivatives between Au electrodes, thermopower,[6] and the conductance[7] can be predictably but modestly controlled using chemical substituents to shift the MOs. Similarly it has been shown that better alignment and thus higher conductance can be achieved by using Pt instead of Au where the higher work function places the Fermi level closer to phenylene's HOMO[8,9] promising as much as an order of magnitude improvement in the conductance. However, for phenylene molecules, obtaining even better alignment is difficult because Pt's chemical potential is rivaled in magnitude only by rare elements such as osmium and selenium.

Hitherto, previous thermopower and conductance measurements have focused primarily on relatively small alkane and phenyl derivatives.[6,7,10−15] Bergfield and Stafford[16] recently predicted that thermopowers exceeding 150 μV/K (on par with inorganic thermoelectric materials) are possible in more highly conjugated molecules. Fullerene molecules are highly conjugated and have additional characteristics necessary to realize high thermopower regimes[17,18] including: (i) small HOMO−LUMO gaps (i.e., 2−3 eV vs 5−10 eV for alkane or phenyl molecules) facilitating chemical potential alignment, (ii) degenerate orbitals attributed to the high symmetry, and (iii) LUMO dominated transport in the bulk, making them the common choice for acceptor in organic photovoltaics.[19]

Single-fullerene conductance measurements (all under UHV) have yielded a wide range of values. Joachim et al.'s pioneering measurements of C_{60} between W and Au electrodes yielded a low conductance of $2.4 \times 10^{-4} \pm 1.2 \times 10^{-4}$ G_0[20] (using an STM at 300 K), but more recent Au−C_{60}−Au[21] (using a mechanical breakjunction at 10 K), Pt−C_{60}−Pt[9] (using a mechanical breakjunction at 300 K), and W−C_{60}−Cu[22] (using an STM at 8 K) junctions have found conductances as high as 0.1, 0.2, and 0.25 G_0. The large spread in high and low conductance values is not surprising as it has been observed that the orientation of the molecules on surfaces strongly affects the alignment and coupling of frontier molecular orbitals with the electronic states of the metal. STM images, experiments, and measurements by Lu et al. on Ag,[23,24] Néel et al. on Cu,[25] and Rogero et al. on Au[26] substrates all support this claim. Specifically, Lu et al. show a distribution of conductance values due to the orientations and contact of the molecule at low temperatures and Rogero et al. show that no preferential orientation is present at 300 K. Some STM techniques, such as the work of Joachim et al. and the work reported herein, sample a wide variety of molecular orientations and contact geometries by making multiple measurements at room temperature, where the thermal energy is sufficient for the molecule to transition between these orientations. This should result in a large spread of conductances as suggested by benzedithiol experiments and theory.[27,28] This is different from the work of Bohler et al.[21] and Kiguchi et al.,[9] which used a mechanical breakjunction to trap one molecule in a unique orientation preserved by low temperatures. Furthermore, this previous work has shown that the conductance of these junctions is dependent on electrode material used suggesting that alignment and coupling of the fullerene's LUMO and the work function of the metal is important.

Herein, we show how this alignment and coupling manifests itself in electronic transport by conducting a systematic study of thermopower and conductance of C_{60}, [6,6]-phenyl-C_{61}-butyric acid methyl ester (PCBM), and C_{70} heterojunctions trapped between Pt, Au, and Ag electrodes. We observe that the trend in thermopower versus metal work function agrees with MO alignment while no trend in conductance is observed which is expected based on the wide range of molecular orientations that are sampled. The weak dependence on orientation is one strength of using thermopower to probe electronic transport in molecular junctions. Finally, this work suggests a new pathway to improve thermoelectric performance by heterostructuring organic and inorganic materials at the nanoscale.

Conductance and thermopower measurements were carried out as previously described in literature[1,2,6,10,11] and illustrated in Figure 1. Details may be found in the Supporting Information but to summarize: a 1 mM dichlorobenzene solution containing a fullerene derivative (i.e., either C_{60}, PCBM, or C_{70}) is first drop cast onto a freshly cleaned and annealed Au substrates and the

dx.doi.org/10.1021/nl2014839 |*Nano Lett.* XXXX, XXX, 000–000

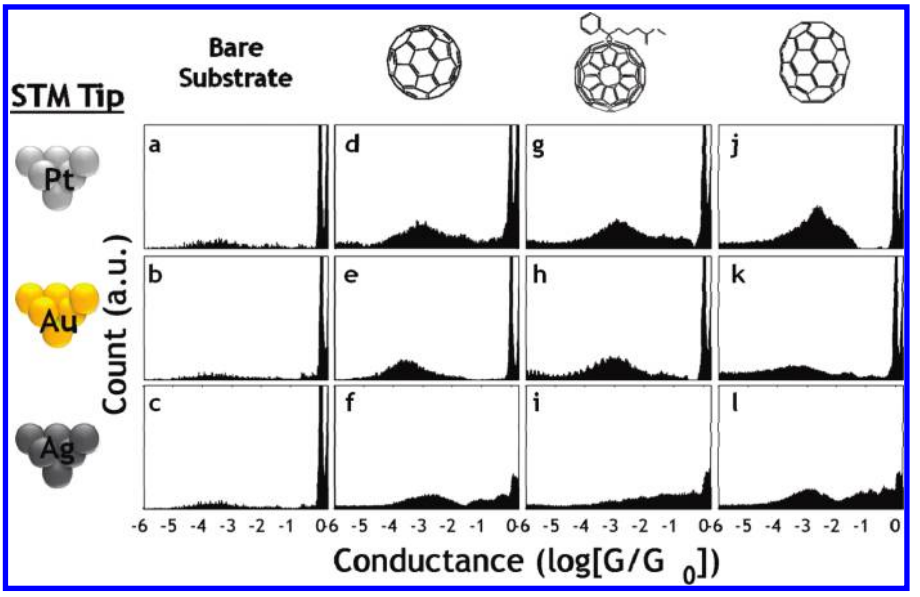

Figure 2. Conductance histograms. A matrix summarizing the normalized conductance data for ~2000 consecutive junctions organized in columns by fullerene derivative and rows by electrode composition. The first column (a−c) represents the conductance of tip and substrate in the absence of molecules showing the recognizable 1 G_0 peak. Log(G/G_0) bin size is −0.006 (i.e., 1000 bins per 6 decades). Vertical scale reduced to emphasize low conductance histograms.

solvent is permitted to evaporate. A modified STM is used to contact the molecules where the STM tip material varies between Pt, Au, and Ag. Au substrates were used for all measurements as we suspect that the malleability of Au is necessary to create junctions of acceptable duration for measurement. Special care was taken to prepare the tips and keep them free of contamination (see Supporting Information). Au and Pt tips were cleaned in a piranha bath and under an oxygen plasma. The Ag tips were cleaned in a hydrogen torch that also served to reduce oxide or sulfide formation back to pure metal. Energy dispersive X-ray spectroscopy (EDS) in a scanning electron microscope confirms the purity before and after use showing that no detectable amounts of substrate Au cross contaminated the Ag or Pt tips. It further confirms that no detectable contaminants such as organics, oxides, or sulfides formed on the Ag tip during the tip preparation and/or measurement time.

For conductance measurements, a 100 mV bias is applied between the metal tip and the Au substrate. More than 2000 junctions are formed during repeated approach and withdraw sequences while continuously measuring the conductance. Lack of metal cross-contamination during these sequences likely results from our choice of a low threshold conductance (~6 G_0) that initiates the withdraw sequence. Steps in conductance are observed corresponding to 1D metal−metal junctions at 1 G_0 and steps corresponding to molecules are observed below 1 G_0. Theory predicts that the value of 1 G_0 is independent of the material properties and hence should be consistent for all tips,[2,29,30] however, noninteger variations in this value have been experimentally observed.[31] To better distinguish between the steps in conductance and the exponential decay of tunneling currents, only data points possessing a negative curvature in conductance traces are selected for histograms as described in detail in the Supporting Information.

For thermopower measurements, the Au substrate is heated to a temperature ΔT above the temperature of the metal tip. The tip approaches the surface while the conductance of the junction is

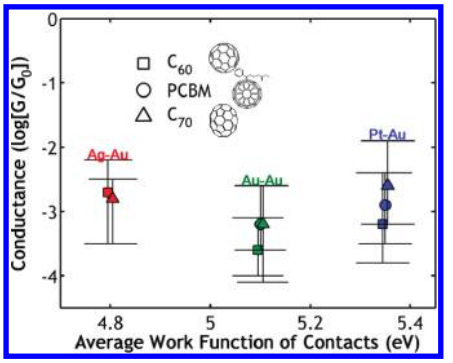

Figure 3. Conductance versus work function. The observed conductance of C_{60}, PCBM, and C_{70} junctions is plotted vs the average work function of the electrodes (nominal work functions: Ag ≈ 4.5 eV, Au ≈ 5.1 eV, and Pt ≈ 5.6 eV. A slight *x*-offset has been applied so individual error bars could be distinguished). Error bars represent the fwhm of the observed lowest conductance peaks in the histograms. The large spread suggests that conductance of fullerene junctions may vary widely, possibly due to molecular orientations in the junction.

monitored with a current amplifier. When a threshold conductance corresponding to a few molecules in the gap is met, the current amplifier is disconnected and a voltage amplifier is connected to measure the resulting thermoelectric voltage generated in the junction as the tip withdraws. Upon breaking the junction, the voltage amplifier is disconnected and the current amplifier is reconnected for the next approach sequence. In this manner >500 thermopower junctions and voltage histograms are constructed at each ΔT. Since the threshold conductance is less than 1 G_0, metal−metal junctions are not formed and metal−metal cross contamination is unlikely.

The conductance histograms are found in Figure 2a-l. In Figure 2, the first row (a,d,g,j), second row (b,e,h,j), and third row (c,f,i,l) represent the conductance with Pt, Au, and Ag STM

dx.doi.org/10.1021/nl2014839 |*Nano Lett.* XXXX, XXX, 000–000

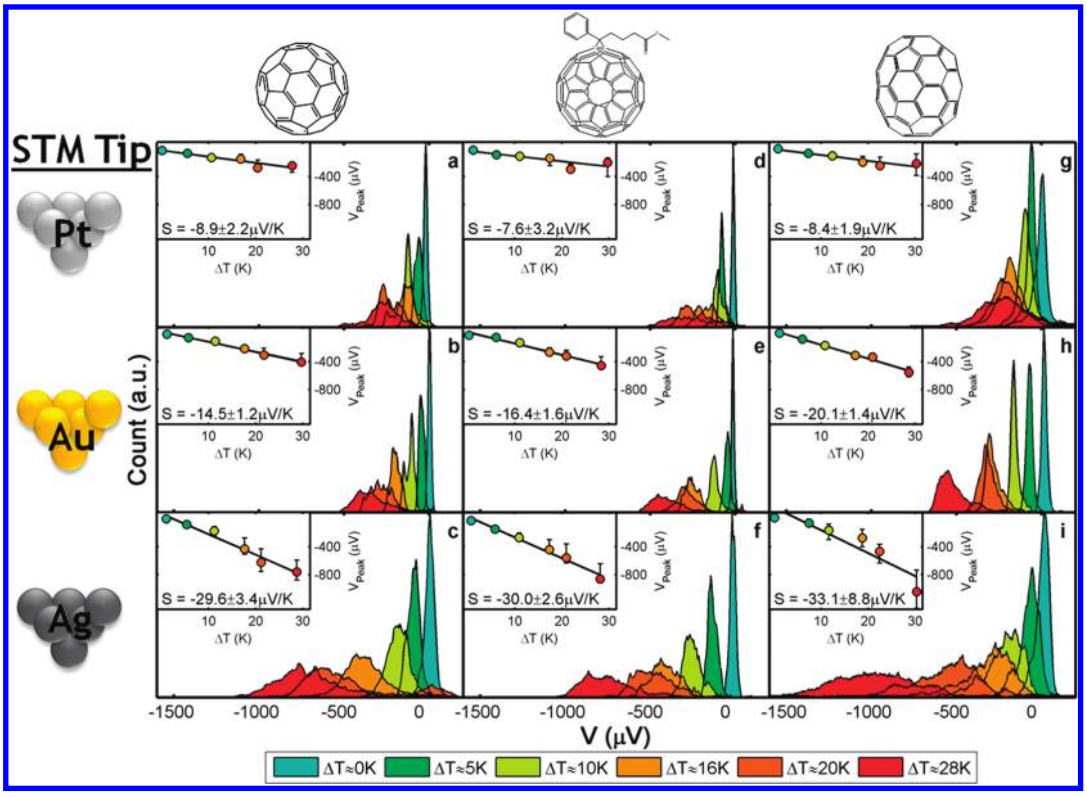

Figure 4. Thermopower histograms and linear regressions. A matrix summarizing the thermopower data is organized in columns by fullerene derivative and rows by electrode composition. The normalized voltage histograms compile data for ~500 consecutive junctions at each ΔT, without preselection. Insets show the voltage histogram peaks as a function of ΔT, where the error bars represent the fwhm of the associated histogram. The voltage peaks vary linearly with ΔT for all junction combinations. The slope of the linear regression defines the thermopower where the reported error is the 95% confidence interval of the regression.

tips all with a Au substrate, respectively. The first column represents the junction conductance in the absence of any fullerene molecules (a,b,c); only a single peak corresponding to the quantum of conductance is visible near 1 G_0. The second column (d,e,f), third column (g,h,i), and fourth column (j,k,l) represent the conductance of C_{60}, PCBM, and C_{70} respectively. Note the large variation in the apparent molecular conductance peaks. Prior studies suggest that variation comes from the multiple orientations that fullerenes take on the electrodes. This variation is compounded by the use of different tip and substrate materials (and thus different crystal direction and bonding geometries) in our study. While the spread in the conductance makes reporting a single fullerene conductance value challenging, the peak of the smallest observed conductance and the fwhm of that peak (when present) have been plotted against the average work function of the tip and substrate in Figure 3. Using the average work function of dissimilar contacts, Beebe et al. identified trends in conductance of alkanethiol junctions.[32,33] In contrast, Figure 3 shows that we observe no clear trend in the conductance.

Upon inspection of the histograms, the conductance profile using the Ag tip differs from those profiles where a Au or Pt tip is used. We attribute this to the breaking of the LUMO's degeneracy (which is 6-fold degenerate for C_{60}) when coupled to the Ag surface in certain orientations, as first recorded by Lu et al.[23,24] High symmetry of some fullerenes creates multidegenerate LUMO. This degeneracy is broken when the fullerene bonds to Ag, resulting in one orbital being pushed to lower energies and becoming more closely aligned with the Fermi level of Ag. This results in higher observed conductance and provides an explanation for the broadening of the G_0 peak that occurs with a Ag tip. Alternatively, assuming that the degeneracy is not broken, the conductance of a single-orbital would then simply be multiplied by the degeneracy to give the conductance of the molecule. The thermopower, however, will not be affected by the degeneracy as it is the slope of the transmission function normalized to the transmission function as shown in eq 2. These complications make interpreting trends in conductance more difficult.

Thermopower measurements show a clear trend with respect to the work function of the electrodes. Voltage histograms and the inferred thermopowers are shown in Figure 4a−i, where the rows are for Pt, Au, and Ag tips, and the columns are for C_{60}, PCBM, and C_{70} molecules. In the absence of molecules, a small thermoelectric voltage corresponding to the Seebeck effect of the metal STM tip, only occurs when the STM tip crashes into the substrate. Seebeck measurements of Ag, Au, Pt, and Cu STM tips with a Au substrate (see Supporting Information) show that our measurement always yields the thermopower of the tip material upon contact. In the presence of fullerene molecules, the measured thermopower is far larger in magnitude, indicating that the measured thermopower is a characteristic of the fullerene junction, rather than the metal electrodes alone. When the fullerenes are present, the histogram peak values, V_{peak} are plotted as a function of ΔT in the insets, where the error bars represent the fwhm of the voltage histograms. The slope of the least-squares linear fit is the junction thermopower S and the 95% confidence interval in slope is the error in S (reported in the

dx.doi.org/10.1021/nl2014839 |*Nano Lett.* XXXX, XXX, 000–000

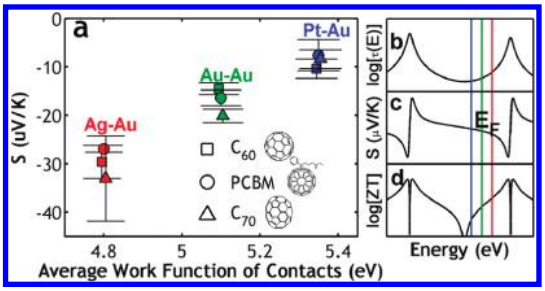

Figure 5. Thermopower versus work function and its effect on ZT. (a) The observed thermopower of C_{60}, PCBM, and C_{70} junctions is plotted vs the average work function of the electrodes (nominal work functions: Ag ≈ 4.5 eV, Au ≈ 5.1 eV, and Pt ≈ 5.6 eV. A slight *x*-offset has been applied so individual error bars could be distinguished). A clear trend indicates that the lower work function electrodes result in higher negative thermopowers. A Lorentzian depiction of the transmission function (b) and the related energy dependent thermopower (c) show that the increasingly negative thermopower results from improved alignment between Fermi level, E_F, and the fullerene LUMO. Blue, green, and red vertical lines approximate the position of the E_F for Pt−Au, Au−Au, and Ag−Au junctions. (d) The ZT associated with the transmission function and thermopower in (b) and (c) increases dramatically when E_F is aligned with the LUMO using low work function electrodes.

insets to Figure 4a−i). All of the molecules demonstrated negative *S*, indicating that the Fermi level of the electrodes was more closely aligned with the LUMO further confirming that these semiconducting molecules behave as electron acceptors (i.e., n-type). The magnitude of *S* is related to the alignment of the Fermi level and the LUMO. Therefore, if the electrode work function decreases, then the magnitude of *S* should increase, as the Fermi level aligns more closely with the LUMO as shown in Figure 5a. As expected, as the average work function of the contacts decreases, the Fermi level moves closer to the LUMO of the molecules resulting in higher *S*.

Generic Lorentzian descriptions of $\tau(E)$ can describe our measurements of thermopower. In this description, the transmission function can be written as

$$\tau(E) = \sum_{i=1}^{N} \frac{4\Gamma_{i,1}\Gamma_{i,2}}{(\Gamma_{i,1} + \Gamma_{i,2})^2 + 4(E - E_i)^2} \quad (3)$$

where, E_i are the MO energies and $\Gamma_{i,1}$ and $\Gamma_{i,2}$ are the broadenings of the i^{th} MOs due to coupling with electrodes 1 and 2. The transmission probability is peaked when the chemical potential aligns well with the energy of the MOs. Figure 5b−d shows a cartoon of how the Lorentzian descriptions of $\tau(E)$ should affect *S* and therefore increase ZT. Observations that *S* grows more negative with reduced work function are consistent with the Fermi level moving toward a position of higher slope on the transmission function (eq 3). The vertical blue, green, and red lines in Figure 5b−d represent the position of E_F for Pt−Au, Au−Au, and Ag−Au electrodes. Also from this description one may expect that an increase in conductance should also strictly occur since the conductance is directly proportional to $\tau(E)$. However, this trend need not be true especially if the coupling terms (i.e., $\Gamma_{i,1}$ and $\Gamma_{i,2}$) associated with each MO are not constant between different tip−molecule−substrate permutations. To illustrate this, consider a transmission function that is dominated by one MO, (e.g., the LUMO), in the weak coupling limit $(\mu - E_{LUMO})^2 \gg (\Gamma_{LUMO,1} + \Gamma_{LUMO,2})^2$. Hence, the conductance and thermopower can be approximated as

$$G \approx \frac{8e^2}{h} \frac{\Gamma_{LUMO,1}\Gamma_{LUMO,2}}{(\Gamma_{LUMO,1} + \Gamma_{LUMO,2})^2 + 4(\mu - E_{LUMO})^2} \propto \frac{\Gamma_{LUMO,1}\Gamma_{LUMO,2}}{(\mu - E_{LUMO})^2} \quad (4)$$

and, given that Γ varies weakly with energy

$$S \approx \frac{8\pi^2 k_B^2 T}{3e} \frac{(\mu - E_{LUMO})}{(\Gamma_{LUMO,1} + \Gamma_{LUMO,2})^2 + 4(\mu - E_{LUMO})^2} \propto \frac{1}{(\mu - E_{LUMO})} \quad (5)$$

In other words, the conductance depends strongly on these coupling terms while thermopower depends only on the relative alignment of energy levels.[28] Trapping the fullerenes between different metal contacts illustrates this concept as multiple orientations, and thus multiple coupling terms, increase the spread in the data as discussed earlier.[23−26]

We demonstrate the first molecular thermoelectric measurements of fullerene molecules (i.e., C_{60}, PCBM, and C_{70}) trapped between electrodes of differing material (i.e., Pt, Au, Ag). We show that while the electronic conductance is highly varying, which is attributed to the multiple orientations and electrode coupling of molecules between the junctions, the thermopower is a robust measurement and can be predictably controlled by selecting the appropriate electrode material for energy level alignment based upon the work function of the electrodes. Furthermore, this is the first observation of negative (n-type) thermopower for single-molecule heterojunctions and is the highest single-molecule heterojunction thermopower recorded to date of −33 μV/K in comparison to a Au−Au junction thermopower of ∼2 μV/K or [1,4]-benezenedithiol thermopower of ∼8 μV/K. This alone results in a substantial improvement to ZT and suggests that organic dopants at inorganic interfaces can lead to further enhancements of thermoelectric efficiency.

■ ASSOCIATED CONTENT

Supporting Information. Substrate and tip preparation, STM conductance measurements, and STM thermopower measurements. This material is available free of charge via the Internet at http://pubs.acs.org.

■ AUTHOR INFORMATION

Corresponding Author

*E-mail: (R.A.S.) segalman@berkeley.edu; (A.M.) Arun Majumdar: Arun.Majumdar@hq.doe.gov.

Present Addresses

⊥Carnegie Mellon University, Pittsburgh, PA 15213, USA.

Author Contributions

‖Equal contributions and first authorship.

■ ACKNOWLEDGMENT

This work was supported by the DOE-BES Thermoelectrics program at Lawrence Berkeley National Laboratories. S.K.Y.

dx.doi.org/10.1021/nl2014839 |*Nano Lett.* XXXX, XXX, 000–000

would also like to gratefully acknowledge a fellowship from the John and Fannie Hertz Foundation.

REFERENCES

(1) Reddy, P.; Jang, S. Y.; Segalman, R. A.; Majumdar, A. *Science* **2007**, *315* (5818), 1568–1571.
(2) Malen, J. A.; Yee, S. K.; Majumdar, A.; Segalman, R. A. *Chem. Phys. Lett.* **2010**, *491*, (4−6), 109−122.
(3) Song, H.Reed, M. A.Lee, T.*Adv. Mater.* **2011**, *23* (14), 1583−1608.
(4) Jonson, M.; Mahan, G. D. *Phys. Rev. B* **1980**, *21* (10), 4223.
(5) Mahan, G. D.; Sofo, J. O. *Proceedings of the National Academy of Sciences of the United States of America* **1996**, *93* (15), 7436–7439.
(6) Baheti, K.; Malen, J. A.; Doak, P.; Reddy, P.; Jang, S. Y.; Tilley, T. D.; Majumdar, A.; Segalman, R. A. *Nano Lett.* **2008**, *8* (2), 715–719.
(7) Venkataraman, L.; Park, Y. S.; Whalley, A. C.; Nuckolls, C.; Hybertsen, M. S.; Steigerwald, M. L. *Nano Lett.* **2007**, *7* (2), 502–506.
(8) Geng, W. T.; Jun, N.; Takahisa, O. *Appl. Phys. Lett.* **2004**, *85* (24), 5992–5994.
(9) Manabu, K. *Appl. Phys. Lett.* **2009**, *95* (7), 073301.
(10) Jang, S. Y.; Reddy, P.; Majumdar, A.; Segalman, R. A. *Nano Lett.* **2006**, *6* (10), 2362–2367.
(11) Malen, J. A.; Doak, P.; Baheti, K.; Tilley, T. D.; Segalman, R. A.; Majumdar, A. *Nano Lett.* **2009**, *9* (3), 1164–1169.
(12) Venkataraman, L.; Klare, J. E.; Nuckolls, C.; Hybertsen, M. S.; Steigerwald, M. L. *Nature* **2006**, *442* (7105), 904–907.
(13) Venkataraman, L.; Klare, J. E.; Tam, I. W.; Nuckolls, C.; Hybertsen, M. S.; Steigerwald, M. L. *Nano Lett.* **2006**, *6* (3), 458–462.
(14) Xiao, X. Y.; Xu, B. Q.; Tao, N. J. *Nano Lett.* **2004**, *4* (2), 267–271.
(15) Xu, B. Q.; Tao, N. J. J. *Science* **2003**, *301* (5637), 1221–1223.
(16) Bergfield, J. P.; Stafford, C. A. *Nano Lett.* **2009**, *9* (8), 3072–3076.
(17) Kroto, H. W.; Allaf, A. W.; Balm, S. P. *Chem. Rev.* **1991**, *91* (6), 1213–1235.
(18) Kroto, H. W.; Heath, J. R.; O'Brien, S. C.; Curl, R. F.; Smalley, R. E. *Nature* **1985**, *318* (6042), 162–163.
(19) Yu, G.; Gao, J.; Hummelen, J. C.; Wudl, F.; Heeger, A. J. *Science* **1995**, *270* (5243), 1789–1791.
(20) Joachim, C.; Gimzewski, J. K.; Schlittler, R. R.; Chavy, C. *Phys. Rev. Lett.* **1995**, *74* (11), 2102–2105.
(21) Bohler, T.; Edtbauer, A.; Scheer, E. *Phys. Rev. B: Condens. Matter* **2007**, *76* (12), 125432.
(22) Neel, N.; Kroger, J.; Limot, L.; Frederiksen, T.; Brandbyge, M.; Berndt, R. *Phys. Rev. Lett.* **2007**, *98*, 065502.
(23) Lu, X. H.; Grobis, M.; Khoo, K. H.; Louie, S. G.; Crommie, M. F. *Phys. Rev. Lett.* **2003**, *90*, 096802.
(24) Lu, X. H.; Grobis, M.; Khoo, K. H.; Louie, S. G.; Crommie, M. F. *Phys. Rev. B* **2004**, *70*, 115418.
(25) Neel, N.; Kroger, J. r.; Limot, L.; Berndt, R. *Nano Lett.* **2008**, *8* (5), 1291–1295.
(26) Rogero, C.; Pascual, J. I.; Gomez-Herrero, J.; Baro, A. M. *J. Chem. Phys.* **2002**, *116* (2), 832–836.
(27) Quek, S. Y.; Venkataraman, L.; Choi, H. J.; Loule, S. G.; Hybertsen, M. S.; Neaton, J. B. *Nano Lett.* **2007**, *7* (11), 3477–3482.
(28) Malen, J. A.; Doak, P.; Baheti, K.; Tilley, T. D.; Majumdar, A.; Segalman, R. A. *Nano Lett.* **2009**, *9* (10), 3406–3412.
(29) Klitzing, K. v.; Dorda, G.; Pepper, M. *Phys. Rev. Lett.* **1980**, *45* (6), 494.
(30) Kittel, C.; McEuen, P. *Introduction to Solid State Physics*, 8th ed.; J. Wiley: Hoboken, NJ, 2005; p xix, 680.
(31) Smit, R. H. M.; Noat, Y.; Untiedt, C.; Lang, N. D.; van Hemert, M. C.; van Ruitenbeek, J. M. *Nature* **2002**, *419* (6910), 906–909.
(32) Beebe, J. M.; Engelkes, V. B.; Miller, L. L.; Frisbie, C. D. *J. Am. Chem. Soc.* **2002**, *124* (38), 11268–11269.
(33) Engelkes, V. B.; Beebe, J. M.; Frisbie, C. D. *J. Am. Chem. Soc.* **2004**, *126* (43), 14287–14296.